

New Herbig-Haro Objects associated with Embedded Sources

T.A. Movsessian,^{1*} T.Yu. Magakian,¹ B. Reipurth² and H.R. Andreasyan¹

¹*Byurakan Observatory NAS Armenia, Byurakan, Aragatsotn prov., 0213, Armenia*

²*Institute for Astronomy, University of Hawaii at Manoa, 640 N. Aohoku Place, Hilo, HI 96720, USA*

Accepted XXX. Received YYY; in original form ZZZ

ABSTRACT

We continue to present the results of the Byurakan Narrow Band Imaging Survey (BNBIS). The main goal of this survey is to search for Herbig-Haro (HH) objects and jets in Galactic dark clouds. In this work we present the results of the search in the vicinity of infrared sources that are bright in the WISE survey and embedded in the dark clouds. The survey is performed with the 1 m Schmidt telescope of Byurakan Observatory, lately equipped with a new CCD detector, which allows to obtain one square degree images of the sky in various filters. Narrow-band filters were used to obtain H α and [S II] images, and a medium-width filter was used for the continuum imaging. New HH flows and knots were found near six embedded IR sources, which constitutes a significant proportion of the objects observed. At least two of the newly found HH flows (HH 1226 and HH 1227) lie in isolated dark clouds, thus pointing to active star formation in these regions. Other flows are also located in detached and dense globules or filaments. The length of the HH 1228 flow is about 1 pc; it has also a molecular hydrogen counterpart of the same extension. Coordinates, charts, detailed descriptions and distance estimates are provided. The lower limits of bolometric luminosities of the source stars are typical for low-mass young stellar objects.

Key words: stars: pre-main sequence – infrared: stars – Herbig-Haro objects

1 INTRODUCTION

Since the discovery of Herbig-Haro objects by [Herbig \(1951\)](#) and [Haro \(1952, 1953\)](#), the number of such known objects is now exceeding 1000.¹ These small shock-excited nebulae, visible in low excitation lines, are the optical manifestation of outflow events near young stellar objects, in various stages of evolution, mostly at very early still embedded stages, but also found associated with visible T Tauri stars. Very often HHs appear as a string of knots aligned in a collimated bipolar flow (HH-flow), and sometimes with a bright bow shock located in a terminal working surface. The spatial extent covered by HH-flows ranges up to several parsecs (giant Herbig-Haro flows, [Reipurth, Bally & Devine 1997](#)). The knots inside such flows trace mass accretion episodes, and giant HH flows thus provide a fossil record of the mass loss and accretion history of their sources.

The presence of HH objects is a sign of active star formation in dark clouds ([Reipurth & Bally 2001](#)). Surveys for HH flows have led to the discovery of new star formation regions (SFRs), in particular surveys around small reflection nebulae, compact stellar groupings, and red nebulous objects in dark clouds have proven successful. Recently we started a survey (Byurakan Narrow Band Imaging Survey, or BNBIS) of dark

clouds with the 1 m Schmidt telescope of the Byurakan Observatory, lately equipped with a new CCD detector, which allows to obtain one square degree images of the sky in various filters. The main goal of this survey is the search for HH objects and jets in Galactic dark clouds. The survey is a continuation of a search for HH objects that was started with the 2.6 m telescope of Byurakan observatory more than 20 years ago ([Magakian & Movsessian 2021](#)), but with a significantly larger field of view. As a first success the Mon R1 association, where several new HH objects and outflow systems were discovered ([Movsessian et al. 2021a](#)), should be mentioned.

In this article we provide data on new HH knots and flows in the vicinity of bright embedded infrared sources with energy distributions typical of young stellar objects.

2 OBSERVATIONS AND DATA REDUCTION

The images were obtained in 2020–2022 with the 1-m Schmidt telescope of Byurakan observatory and a 4K \times 4K Apogee (USA) liquid-cooled CCD camera as a detector with a pixel size of 0.868'' and field of view of about 1 square degree ([Dodonov et al. 2017](#)). Narrow-band filters centered on 6560 Å and 6760 Å, both with a FWHM of 100 Å, were used to obtain H α and [S II] images, respectively. A medium-width filter, centered on 7500 Å with a FWHM of 250 Å, was used for the continuum imaging. A log of observations is presented in Table 1.

* E-mail: tigmov@web.am, tigmag@sci.am

¹ The catalogue of Herbig-Haro objects is maintained by Bo Reipurth.

A dithered set of 5 min exposures was obtained in each filter. Effective exposure time in $H\alpha$ equaled 5100 sec, in $[S\ II]$ 7200 sec and in the continuum 1800 sec. Images were reduced in the standard manner using an IDL² package developed by S. Dodonov (SAO RAS), which includes bias subtraction, cosmic ray removal, and flat fielding using a “superflat field”, constructed from several images.

The search for HH objects was done with the classic technique, suggested in 1975 by van den Bergh (1975), by comparison of $H\alpha$, $[S\ II]$ and I-continuum images. It is based on the characteristic of HH objects strength of $[S\ II]$ emissions, which often is comparable with that of $H\alpha$. To identify probable HH knots we blinked the images, obtained in various wavelengths and also checked all suspicious objects on the images of the PanSTARRS survey. Over the years, this approach has been shown to reliably identify HH objects in the overwhelming majority of cases.

3 RESULTS

3.1 Sample selection criteria

In the initial stage of the survey we chose as targets young stellar objects associated with small reflection nebulae, primarily with a characteristic cone shape. Later the survey was expanded with a search in the vicinities of selected far-infrared sources in little-known small dark clouds and globules. Preliminary results for several fields were shown during a conference in Byurakan (Movsessian et al. 2021b). For the present paper we surveyed embedded IR sources with characteristic SEDs and specific positions in color-color diagrams.

A list of the detected outflows and their potential sources is presented in Table 2. It contains their HH numbers, coordinates, IRAS or 2MASS names of the probable sources, distances and position angles of knots from the sources as well as lower limits to lengths of the flows. In the following we describe results for each flow separately in order of right ascension.

3.2 Description of individual objects

3.2.1 IRAS 23591+4748 and the RNO 150 field

IRAS 23591+4748 is a Class I young stellar object with signs of activity (Connelley & Greene 2010, 2014). The star is visible at both optical (Gaia DR3 393299436722321664) and infrared (2MASS J00014325+4805189) wavelengths. It is located near the edge of the isolated dark cloud CB 248 (Clemens & Barvainis 1988). Connelley et al. (2009) found it to be a close binary with about 1'' separation. Its distance determined in Gaia DR3 is about 380 ± 16 pc.

A small and very red nebulous object is located about 43'' north of IRAS 23591+4748 near the center of a dark globule. Almost certainly this nebulous patch, which is visible even on DSS charts, is the RNO 150 object, because it matches well the description in the list of Cohen (1980), but the coordinates provided by Cohen are not precise.

Our observations indicate the HH nature of this object, which is visible both in $H\alpha$ and $[S\ II]$ images while lacking

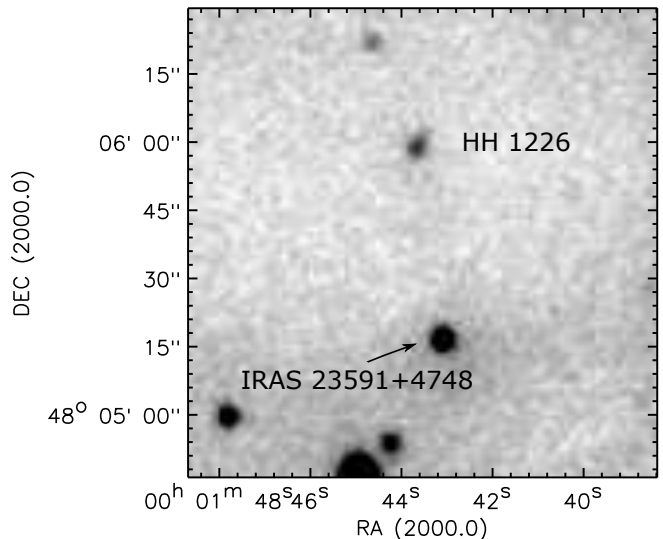


Figure 1. IRAS 23591+4748 and RNO 150 (i.e. HH 1226) as seen in an $H\alpha$ image (all images in this paper, unless otherwise specified, are obtained with the 1 m Byurakan Schmidt telescope).

in continuum emission (Fig.1). In both images one can see a faint short tail, directed to NW, which is distinctly brighter in $H\alpha$. We here label this object as HH 1226.

It should additionally be noted, that HH 1226 can be seen in the K band image of 2MASS survey as well as in W2 (4.6 μm) band of unWISE survey. This indicates the presence of H_2 emission in the object.

3.2.2 The IRAS 01166+6635 field

IRAS 01166+6635 is a very red star visible in PanSTARRS i images. It is bright at near-infrared and especially at mid-infrared wavelengths (it is listed as 2MASS 01200392+6651358 and WISE J012003.93+665135.9). The source is associated with a faint cone-shaped reflection nebula oriented in a N-S direction, 10'' in length, which is well seen in our continuum and $H\alpha$ images. It is located near the center of the isolated dark cloud TGU 829 (Dobashi et al. 2005) or Dobashi 3782 (Dobashi 2011). This nebula is also visible in the near-IR range, with smaller dimensions and oriented to the south-east (Connelley et al. 2007). At a distance of 37'' to the south from this source we found a conspicuous HH object, right on the axis of the optical reflection nebula. It is elongated in a northern direction for about 6'' and consists of a compact leading knot, seen in $H\alpha$ and $[S\ II]$, and a diffuse trail, visible mostly in $H\alpha$. This HH knot was discovered independently in the IGAPS survey; its appearance and kinematics are described in a recent paper (Greimel et al. 2021). Detailed examination reveals the existence of another small emission knot, brighter in $[S\ II]$, near the southern edge of the nebula and about 12'' from the central star. Our $[S\ II]$ images also show enhanced brightness in the 2'' zone just to the south from the brightness maximum in the reflected light (which definitely contains significant part of the reflected stellar $H\alpha$ emission) - see Fig.2, right panel. This might suggest the existence of a jet near the star, which is not visible in the optical. We label the separate knots as HH 1227 A, B and C.

As one can see, the IR source (marked by cross in Fig.2,

² IDL is a trademark of L3Harris Geospatial Solutions.

Table 1. Log of observations

Field	H α	Obs. date [S II]	Continuum
IRAS 23591+4748 (RNO 150)	25.08.2020	26.08.2020	25.08.2020
IRAS 01166+6635	18.12.2020	20.13.2020	18.12.2020
LkH α 101	13.10.2020	14.10.2020	13.10.2020
2MASS 06590141–1159424 (RNO 80)	11.02.2021	05.03.2021	11.02.2021
IRAS 19219+2300	12.09.2021	20.06.2022	12.09.2021
IRAS 20472+4338	18.07.2020	18.07.2020	18.07.2020

Table 2. List of newly discovered HH objects

HH knot	RA (2000.0) h m s	Dec (2000.0) ° ' "	IR source	r''	P.A.°	length (pc)
HH 1226 (RNO 150)	00 01 44.1	+48 06 01	IRAS 23591+4748	43	11	0.08
HH 1227 C	01 20 02.9	+66 51 00	} IRAS 01166+6635	37	} 189	0.15
HH 1227 B	01 20 03.7	+66 51 27		9		0.04
HH 1227 A	01 20 03.8	+66 51 33		4		0.02
HH 1228 A	04 30 42.8	+35 26 16		207		175
HH 1228 B	04 30 42.6	+35 26 06	} WISEA J043041.15+352941.4	221	175	0.57
HH 1228 C	04 30 42.9	+35 25 36		247	175	0.63
HH 1228 D	04 30 44.1	+35 24 50		297	172	0.76
HH 1228 E	04 30 48.0	+35 23 27		385	168	0.99
HH 1229 (RNO 80)	06 59 00.1	–12 00 15		2MASS 06590141–1159424	38	216
HH 1230	19 24 03.8	+23 06 21	IRAS 19219+2300	40	107	0.10
HH 1231 A	20 48 56.8	+43 50 03	} IRAS 20472+4338	33	} 255	0.14
HH 1231 B	20 48 52.5	+43 49 57		82		0.36

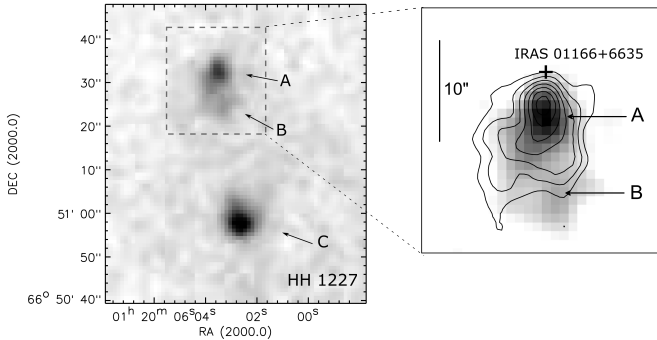


Figure 2. Left: the nebula, connected with IRAS 01166+6635 source and its HH flow (HH 1227 A, B and C); H α + [S II] image. Right: an enlarged part of the cometary nebula, as seen in continuum (isolines) and in H α + [S II] emission (greyscale). The spots of enhanced line emission, marked as A and B, do not coincide with the details of the image in continuum.

right panel) is offset to the north from the tip of the reflection nebula because of the increased extinction toward the star. The same effect is seen in the RNO 80 object (see below).

We did not find any indications of H $_2$ emission from the HH 1227 flow in the images of 2MASS and unWISE surveys.

In the paper by Greimel et al. (2021) a kinematical distance of 240 pc, estimated from CO and H $_2$ O radio observations by Wouterloot & Brand (1989), is given for this cloud. On the other hand, the same CO survey gives for IRAS 01160+6529, which is located only one degree in angular distance from IRAS 01166+6635, several kinematic

estimates, including 830 and 570 pc. Since the catalog of Zucker et al. (2020) gives 834 ± 41 pc for the nearby L 1307 dark cloud, estimated directly from *Gaia* trigonometric parallaxes, 830 pc seems a more reasonable value for the distance of IRAS 01166+6635. This value yields 0.15 pc for the projected length of the HH 1227 flow.

3.2.3 WISEA J043041.15+352941.4

North of the LkH α 101 star forming region (see the review of Andrews & Wolk 2008) there are a number of nebulous stars, surrounded by wisps of dark matter, which never have been studied in detail. In particular, no HH objects were found in this region. Our observations have identified several patches of what appears to be collisionally excited emission in the area of the small reflection nebula around the 12^m star Gaia DR3 173369863892701312, separated from LkH α 101 by a dark lane, which is part of LDN 1482.

One of these knots (C) is particularly bright (see Fig.3) and has an oblong shape, oriented perpendicularly to the probable direction of the flow. It has also a small round appendage. Other four emission patches are very faint.

The comparison of our data with a 4.6 μ m image of the unWISE survey confirmed the reality of all knots as well as the presence of H $_2$ emission in them. There is no obvious source of this flow (which we have labeled HH 1228) at either optical or near-IR wavelengths. However, tracing the flow in a northerly direction, one can find in allWISE images a very red object WISEA J043041.15+352941.4, not detected even in the 2MASS survey. This source lies about 15' to the NNW from LkH α 101.

Analysing the images of the same field in the Spitzer mid-

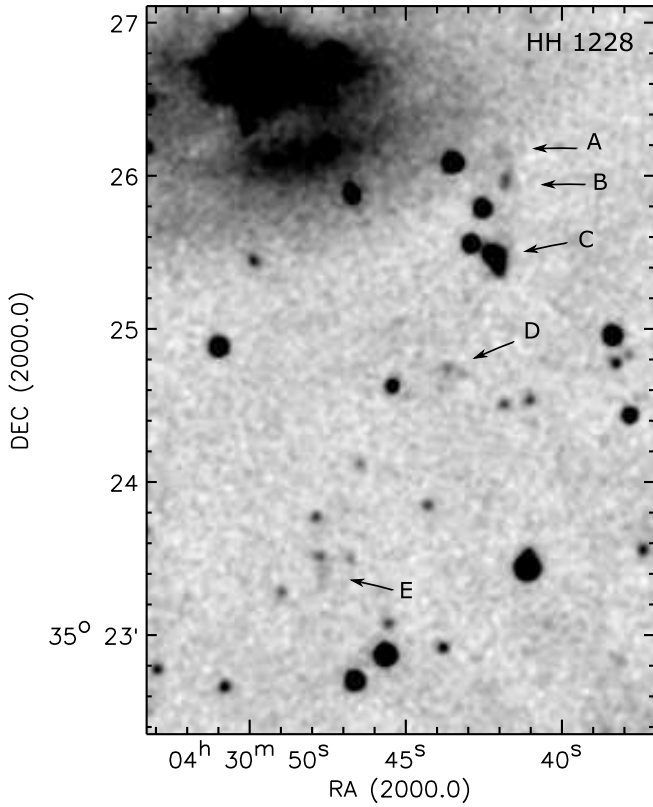


Figure 3. $H\alpha + [SII]$ image of the HH 1228 flow, located to the north of LkH α 101. Individual knots are marked by letters. The probable driving source WISEA J043041.15+352941.4 is outside of the upper border of this frame.

IR SEIP survey, which have significantly higher resolution, we found that all HH knots of the flow indeed are well visible on the 3.6 and 4.5 μm images. On Fig.4, where the H_2 condensations are marked by numbers, object “2” corresponds to HH 1228 A+B, object “3” - to HH 1228 C, “4” - to HH 1228 D and “5” - to HH 1228 E. Moreover, on the place of the knot HH 1228 C in H_2 emission we see a well-defined bow-shock, oriented to the south, while the emission near the knot E is more like a bow-shock with the axis pointing to the south-east. Besides, at a distance of 2.5' to the south from WISEA J043041.15+352941.4 on the SEIP images we found one more arcuate knot with the same orientation, which has no optical counterpart (“1” in Fig.4). The images clearly show the IR reflection cometary nebula, illuminated by the WISEA J043041.15+352941.4 source, the axis of which is directed toward the HH 1228 flow and its molecular analogue (see Fig.4, upper side). Thus, we have no reason to doubt that this IR object indeed is the driving source of the HH 1228 flow. If this assumption is correct, then this flow starts near the source at a position angle of 175° but afterwards, near knot C, turns slightly in a direction with position angle 156° .

WISEA J043041.15+352941.4 is included in the survey of young stellar objects in the Gould Belt by Dunham et al. (2015) under the designation SSTgbs J0430411+352941. According to the results of their photometry and modelling after a correction for $A_V=7.5$, this extremely red object has

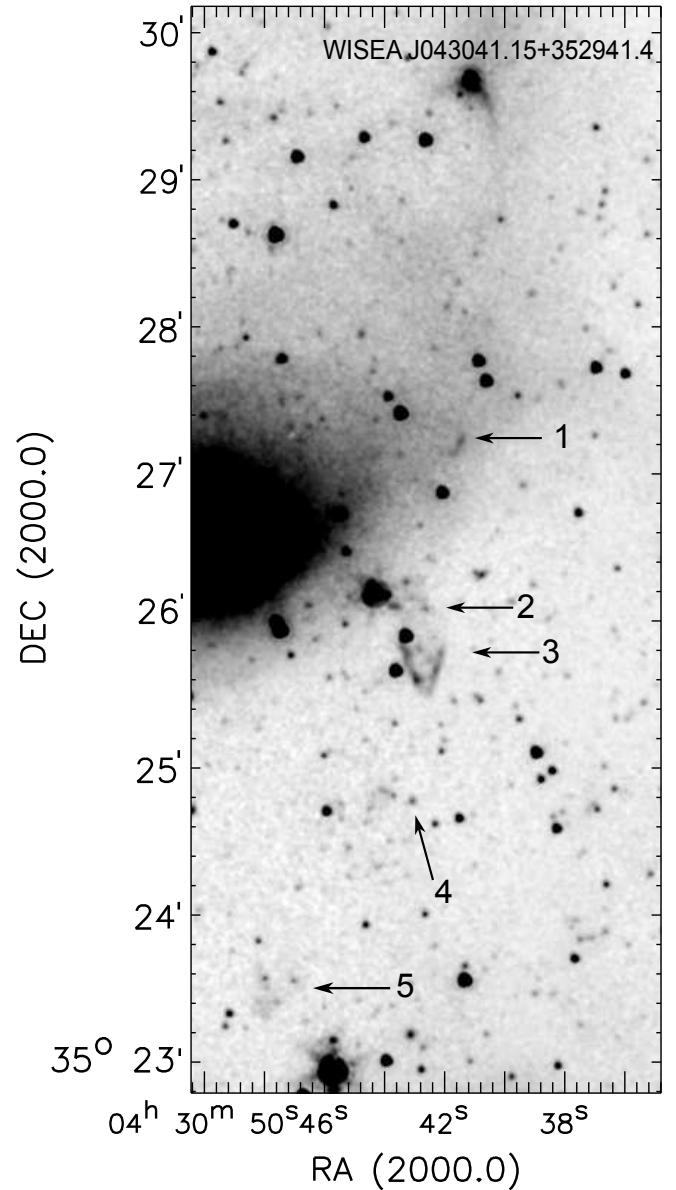


Figure 4. 4.5 μm image of the H_2 flow, associated with HH 1228. Individual components are marked by numbers.

a very low $T_{dust} = 53$ K, while its bolometric luminosity is estimated as $2.5 L_\odot$.

The distance to the LkH α 101 star forming region has been quite controversial (Andrews & Wolk 2008), and even most recent estimates, based on the trigonometrical parallaxes of Gaia DR3, somewhat vary. According to the catalog of Bailer-Jones et al. (2021), LkH α 101 itself has a distance about $\approx 620 \pm 40$ pc (but with significant measurement error: RUWE=2.36), while Dzib et al. (2018) estimated a distance of 535 ± 29 pc for one of the members of the LkH α 101 cluster by VLBA radioastrometry. To understand if the nebulae and dark lanes, located in the northern direction from this star forming region, have the same distance, we checked the Gaia parallaxes of two bright stars illuminating nebulae to the east and to the west of the HH 1228 flow: the above mentioned TYC 2381-482-1 (Gaia DR3 173369863892701312) and 2MASS J04301644+3525217

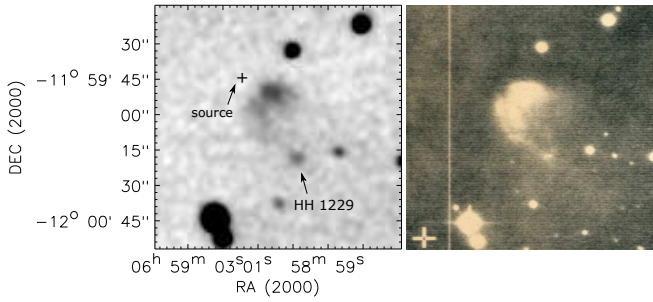


Figure 5. The RNO 80 nebula and the HH 1229 knot, visible on its axis. 1-m Schmidt, H α image (left panel); 3.6-m ESO telescope, broad-band R filter (right panel). The 2MASS 06590141–1159424 source inside the cloud is marked by a cross.

(Gaia DR3 173380579834746112). The distance of both stars in the [Bailer-Jones et al. \(2021\)](#) catalog is very near to 530 pc, in excellent agreement with the radioastrometric distance of the LkH α 101 cluster. Thus, we adopt 530 pc as the distance for the HH 1228 flow. If WISEA J043041.15+352941.4 is indeed the source of this outflow, then its projected length, measured along the flow, will be about 1.0 pc, which makes it the most extended flow in the present sample.

3.2.4 RNO 80 (2MASS 06590141–1159424)

RNO 80 is a faint, nebulous object in the dark cloud Dobashi 5068. It was discovered by [Cohen \(1980\)](#), who described it as a group of faint stars in a common nebula, but no stars can be seen in the optical on PanSTARRS images. The nebula has the appearance of a small cylindrical lobe with a rounded bright edge. The exciting star starts to be visible only in the H band image of the 2MASS survey; in K band it already becomes prominent. As in many similar cases, the infrared star is embedded and offset from the optical nebula which likely represents an illuminated cavity, created by a molecular outflow.

Our images (see Fig.5) reveal a single HH knot (HH 1229), better visible in H α than in the [S II] lines, about 38'' from the central star, and approximately on the symmetry axis of the visible nebula. No other knots, nor signs of a counterflow, have been detected. There are also no traces of an emission jet inside the nebula. In the 4.6 μ m image of the unWISE survey at the place of HH 1229 one can see a faint patch, which indicates the presence of H $_2$ emission.

The RNO 80 field is part of a large star-forming region CMa OB1 + CMa R1. A compact group of stars with H α emission is located about one degree to the west from the center of the main association ([Pettersson & Reipurth 2019](#)), and this is where RNO 80 is located. On the basis of Gaia data the distance of this star forming region was estimated as 1185 pc ([Pettersson & Reipurth 2019](#)). RNO 80 lies in a narrow dark lane that ends near the bright reflection nebula GN 06.56.9.01. The illuminating star of this nebula is Gaia DR3 3045899512500879744, the distance of which, according to [Bailer-Jones et al. \(2021\)](#), is about 1330 pc.

3.2.5 IRAS 19219+2300 field

This infrared source has no optical counterpart, and is located in the dense dark cloud TGU 394P1 or Dobashi 1983

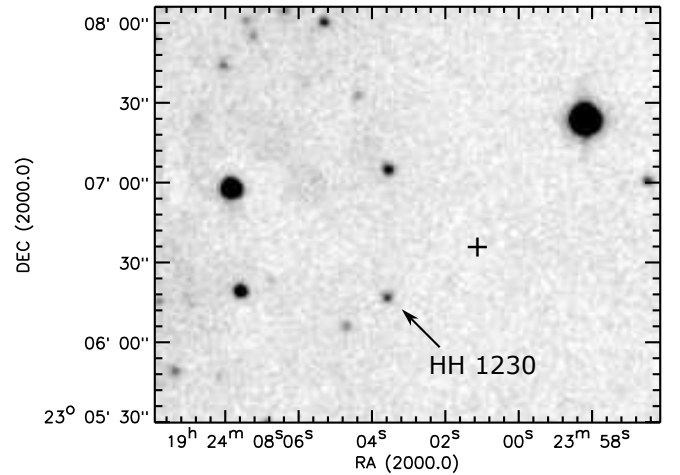


Figure 6. IRAS 19219+2300 (marked by a cross) and the HH 1230 knot. H α image.

([Dobashi et al. 2005](#); [Dobashi 2011](#)). The source is detected in the 2MASS (as 19240107+2306351) and WISE surveys. About 40'' to the west we have found a single compact HH knot (HH 1230) with nearly equal brightness in H α and [S II], for which the IRAS source seems to be the most probable source, since there are not any other suitable objects in the vicinity (Fig.6). We have not found any references to the distance of this cloud. However, on the western side of Dobashi 1983 two nebulous stars can be seen: Gaia DR3 2019298532316094208 and Gaia DR3 2022295079462085632, whose distances, according to the [Bailer-Jones et al. \(2021\)](#) catalog, are both around 530 pc. Thus, we assume this value as the probable distance of the Dobashi 1983 cloud.

In the 4.6 μ m IR image of the unWISE survey, the HH knot is visible and has the appearance of a small bow shock, oriented towards the east. We speculate that HH 1230 may be part of a larger, perhaps partly embedded, flow.

We note that about 2.7' further to the east from the HH 1230 knot we find another bright IR source, IRAS 19221+2300 (2MASS 19241551+2306030), which is also visible in the optical. This star is located at the center of a so far unlisted reflection nebula with a well-defined bipolar structure (Fig. 7). However, the axis of this nebula is nearly orthogonal to the direction to HH 1230; thus it is unlikely to be the exciting source of this object. The central star is listed as Gaia DR3 2019294237343467264. Its astrometric measurements are of very poor quality (RUWE = 5.45), but it appears likely that this object also belongs to the Dobashi 1983 cloud. We have not found convincing evidence for any shock-excited emission in its environment on our wide-field images.

3.2.6 IRAS 20472+4338 field

This deeply embedded source is located within a dark cloud near the western side of the Pelican nebula (IC 5070). It is not detected at optical and near-IR J and H wavelengths and only appears weakly on a 2MASS K -band image, with traces of nebulosity. This field was covered by the Spitzer SEIP survey, where on the 3.6 and 4.5 μ m images one can see a comma-like nebula, which extends $\sim 15''$ from the IRAS 20472+4338 source in P.A. = 56°. Recently [Zhang et al. \(2020\)](#) found in

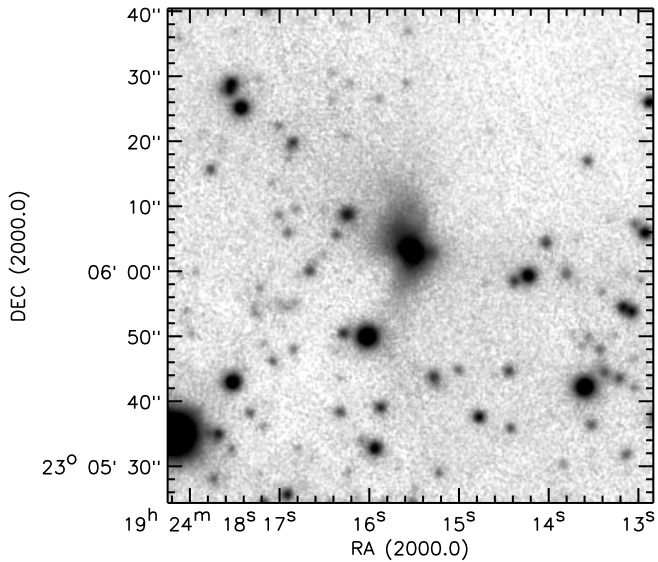


Figure 7. Newly found bipolar nebula. IRAS 19221+2300 coincides with a star in its center. PanSTARRS survey *i* image.

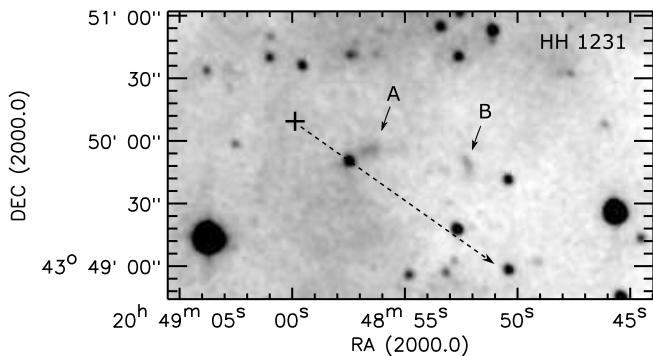


Figure 8. IRAS 20472+4338 (marked by cross) and two nearby HH knots (HH 1231 A and B), visible in $H\alpha$ image. The approximate direction of the CO outflow from IRAS 20472+4338 is shown by dashed line.

^{12}CO evidence of a bipolar molecular outflow from this source (DMOC-0006). The approximate direction of the red lobe of this outflow is shown on Fig.8. Its P.A. (235°) shows that it is directed almost exactly opposite to the IR-nebula, seen near the source.

This region is active in low mass star formation, and a number of HH objects are located further north (Bally & Reipurth 2003). We found two faint HH knots (HH 1231 A and B) in the western direction from IRAS 20472+4338. Along with this source they define a nearly straight line with P.A. = 255° (Fig.8). The HH knots probably lie within the red-shifted lobe of the molecular outflow. Knot A is diffuse and extended over about $10''$. Knot B may have a bow-shape morphology, which is more prominent in [SII]. We did not find evidence of H_2 emission in the images from allWISE and unWISE surveys. Their association to the IRAS 20472+4338 source seems possible but not entirely certain.

The distance of this molecular outflow as well as of the cloud is estimated by Zhang et al. (2020) as 900 ± 100 pc.

Table 3. Minimal bolometric luminosity of the infrared sources

Source	D (pc)	$L(L_\odot)$
IRAS 23591+4748 (RNO 150)	380	1.0
IRAS 01166+6635	240	0.6
WISEA J043041.15+352941.4	530	2.5 ^a
2MASS 06590141–1159424 (RNO 80)	1185	2.3
IRAS 19219+2300	530	2.7
IRAS 19221+2300	530	4.9
IRAS 20472+4338	900	16.4

^aFrom the survey of Dunham et al. (2015).

4 DISCUSSION AND CONCLUSION

The results presented in this paper, as well as data published separately (Movsessian et al. 2022, 2023), show that the survey technique employed here is indeed successful, and new HH knots and flows have been found near a significant part of the embedded IR sources observed. At least two from the newly found HH flows (HH 1226 and HH 1227) lie in isolated dark clouds, thus pointing to active star formation in these regions. Other flows are also located in detached and dense globules or filaments.

The IR sources which drive the newly discovered flows need further study. With the aid of the *VizieR Photometry viewer* we have built spectral energy distributions (SEDs) for six IR sources from our sample (Fig. 9). IRAS 20472+4338 was also observed in two wavebands of the Herschel PACS survey; we added these measurements to its SED. The value of the $100 \mu\text{m}$ flux of this object, as measured by IRAS, is improbably high, judging by the general appearance of its SED; therefore, we excluded it from the final computations. We do not include here the SED for WISEA J043041.15+352941.4, because it can be found in the electronic version of the work of Dunham et al. (2015). For completeness we have also included the IRAS 19221+2300 source at the center of the new bipolar nebula. One can see that all sources have so-called "flat" SEDs, typical for very young objects, with the exception of WISEA J043041.15+352941.4, which, according to Dunham et al. (2015), has a spectral index of about 1.5 with a rising SED, corresponding to a Class I object.

As described in the previous sections, the distances of all objects are now reasonably well known, which allows to estimate the bolometric luminosity of the sources by integrating their SEDs. The values thus obtained are listed in Table 3. Of course, these values are lower estimates, because extinction is not taken into account and, in addition, we do not have the data in the FIR/submm part of the SEDs. As one can see, the objects have luminosities typical for low-mass YSOs, and only the luminosity of IRAS 20472+4338 exceeds $10 L_\odot$.

We have plotted all the IR sources discussed in this paper on a (J-H)/(H-K) color-color diagram (Fig.10), with the exception of WISEA J043041.15+352941.4, which was not detected in the near-IR range. Also in this diagram the regions of Herbig Ae/Be and T Tau stars and of the luminous Class I protostars, according to work of López et al. (2021), are shown. As can be seen in this figure, all of the sources have IR color indices characteristic of YSOs, though they do not correlate with their luminosity or with the shape of their SEDs over the middle IR range. It is remarkable that the ob-

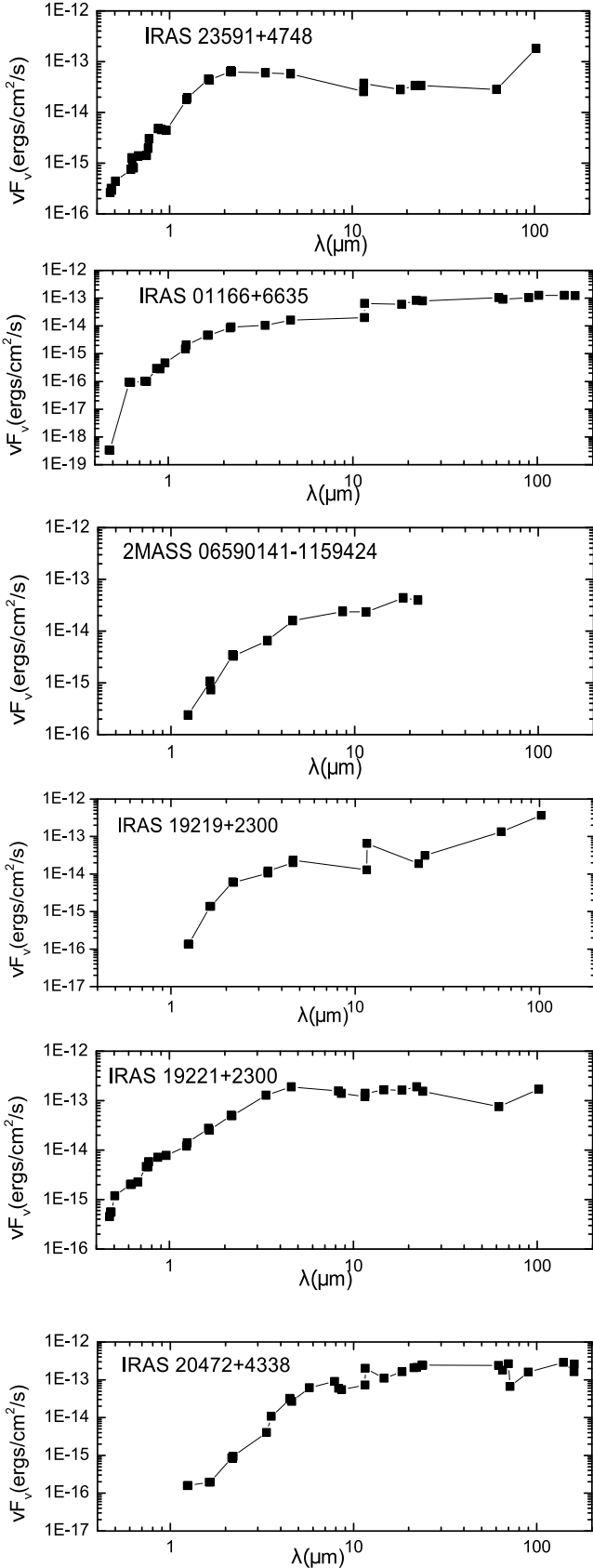


Figure 9. SEDs of the infrared sources, associated with HH flows.

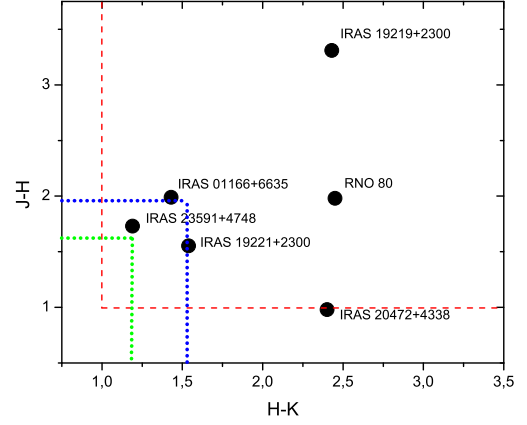


Figure 10. $(J-H)/(H-K)$ diagram for the observed sources. Red rectangle shows the region of Class I sources, blue rectangle of H Ae Be stars, and the green one of T Tau stars.

jects with $J - H$ and $H - K < 1$ are absent in this sample. They all seem to be redder than the typical T Tau stars.

Three of the IR sources from our sample are visible in the optical range; their nature can be further investigated spectroscopically. In fact, a program of long-slit spectroscopy of IR sources of HH flows, discernible also in optical range, for the objects, found in Mon R1 association (Movsessian et al. 2021a) and in other fields, has already started, and some preliminary results were recently presented (Movsessian & Magakian 2023).

ACKNOWLEDGEMENTS

We thank an anonymous referee for helpful comments, which improved the paper.

This work was supported by the RA MES State Committee of Science, in the frame of the research project number 21T-1C031.

This research has made extensive use of *Aladin* sky atlas, *VizieR* catalogue access tool, *VizieR* photometry tool and *SIMBAD* database, which are developed and operated at CDS, Strasbourg Observatory, France. This work has made use of data from the European Space Agency (ESA) space mission Gaia, processed by the Gaia Data Processing and Analysis Consortium (DPAC). Funding for the DPAC is provided by national institutions, in particular the institutions participating in the Gaia MultiLateral Agreement (MLA). The Gaia mission website is <https://www.cosmos.esa.int/gaia>. The Gaia archive website is <https://archives.esac.esa.int/gaia>. This publication makes use of data products from the Two Micron All Sky Survey (2MASS), which is a joint project of the University of Massachusetts and the Infrared Processing and Analysis Center/California Institute of Technology, funded by the National Aeronautics and Space Administration and the National Science Foundation. This publication also makes use of data products from the Wide-field Infrared Survey Explorer (WISE), which is a joint project of the University of California, Los Angeles, and the Jet

Propulsion Laboratory/California Institute of Technology, funded by the National Aeronautics and Space Administration. The images from Spitzer Enhanced Imaging Products program were used via NASA/IPAC Infrared Science Archive <https://www.ipac.caltech.edu/doi/irsa/10.26131/IRSA3>

This paper has been typeset from a $\text{\TeX}/\text{\LaTeX}$ file prepared by the author.

DATA AVAILABILITY

The data underlying this article will be shared on reasonable request to the corresponding author.

REFERENCES

- Andrews, S. M., Wolk, S. J., 2008, in Handbook of Star Forming Regions, Vol.I, (ed. B.Reipurth), ASP Monograph No.4, p. 390
- Bailer-Jones, C. A. L., Rybizki, J., Foesneau, M., Demleitner, M., Andrae, R., 2021, *AJ*, 161, 147
- Bally, J., Reipurth, B., 2003, *AJ*, 126, 893
- Clemens, D. P., Barvainis, R., 1988, *ApJS*, 68, 257
- Cohen, M., 1980, *AJ*, 85, 29
- Connelley, M. S., Greene, T. P., 2010, *AJ*, 140, 1214
- Connelley, M. S., Greene, T. P., 2014, *AJ*, 147, 125
- Connelley, M. S., Reipurth, B., Tokunaga, A. T., 2007, *AJ*, 133, 1528
- Connelley, M. S., Reipurth, B., Tokunaga, A. T., 2009, *AJ*, 138, 1193
- Dobashi, K., Uehara, H., Kandori, R., Sakurai, T., Kaiden, M., Umemoto, T., Sato, F., 2005, *PASJ*, 57, S1
- Dobashi, K., 2011, *PASJ*, 63, S1
- Dodonov S. N., Kotov S. S., Movsesyan T. A., Gevorkyan M., 2017, *Astrophysical Bulletin*, 72, 473
- Dunham, M. M., Allen, L. E., Evans, N. J. et al., 2015, *ApJS*, 220,11
- Dzib, S. A., Ortiz-León, G. N, Loinard, L. Mioduszewski, A. J., Rodríguez, L. F., Medina, S.-N. X., Torres, R. M. , 2018, *ApJ*, 853, 99
- Greimel, R., Drew, J. E., Monguió, M. et al., 2021, *A&A*, 655, A49
- Haro, G., 1952, *ApJ*, 115, 572
- Haro, G., 1953, *ApJ*, 117, 73
- Herbig, G. H., 1951, *ApJ*, 113, 697
- Herbig, G. H., Andrews, S. M., Dahm, S. E., 2004, *AJ*, 128, 1233
- López, R., Riera, A., Estalella, R., Gómez, G., 2021, *A&A*, 548, A57.
- Magakian, T. Yu., Movsessian, T. A., 2021, in *Byurakan Astrophysical Observatory – 75 years of outstanding achievements*, ed. A.G. Mickaelian, Yerevan Edit Print publ., p. 56
- Movsessian, T. A., Magakian, T. Yu., Dodonov, S. V., 2021a, *MNRAS*, 500, 2440
- Movsessian, T. A., Magakyan, T. Yu., Dodonov, S. N., Andreasyan, H. R., 2021, *Comm. Byurakan Astroph. Obs.*, 68, 436
- Movsessian, T. A., Magakian, T. Yu., Andreasyan, H. R., 2022, *Astrophysics*, 65, 193
- Movsessian, T. A., Magakyan, T. Yu., 2023, *Comm. Byurakan Astroph. Obs.*, 70, 49
- Movsessian, T. A., Magakian, T. Yu., Rastorguev, A. S., Andreasyan, H. R., 2023, *Astrophysics*, 66, 52
- Pettersson, B., Reipurth, B., 2019, *A&A*, 630, A90
- Reipurth, B., Bally, J., 2001, *Ann. Rev. Astron. Astrophys.* 39, 403
- Reipurth, B., Bally, J., Devine, D., 1997, *AJ*, 114, 2708
- van den Bergh, S., 1975, *PASP*, 87, 405
- Wouterloot, J. G. A., Brand, J. 1989, *A&AS*, 80, 149
- Zhang, S. , Yang, J., Xu, Y. et al., 2020, *ApJS*, 248, 15
- Zucker, C., Speagle, J. S., Schlafly, E. F., Green, G. M., Finkbeiner, D. P., Goodman, A., Alves, J. 2020, *A&A*, 633, A51